Temperature trends and episodic changes of the middle atmosphere over Logan Utah with consideration to model specification

Troy A. Wynn[a*], Vincent B. Wickwar[b]

[a, b] Center for Atmospheric and Space Sciences (CASS), Utah State University, 4405 Old Main Hill, Logan, UT 84322-4405, USA.

* Corresponding Author. E-mail address: troy.wynn@aggiemail.usu.edu

Abstract: A summary of the linear trends estimated from the USU Rayleigh Lidar (41.74º N, 118ºW) temperature data set. The data set covers a time span from September, 1993 to August, 2003 and an altitude range of 45 to 80 km. The data set includes 584 data points at 45 km to 580 data points at 80 km. Cooling trend profiles are calculated and compared to results from other researchers. Collinearity and bias are also considered as issues that could affect the regression results. Also considered is the possibility that the Mt. Pinatubo eruption has influenced temperature trend estimates. This is important because the Pinatubo-related mesosphere temperature response occurred about the time the USU lidar came on line, which could be affecting our trend estimates. A visual comparison of the annual and semiannual oscillations are also presented.

1 Introduction

A theoretical connection between elevated atmospheric CO_2 levels and increased global temperatures has existed for over 100 years (Callendar, 1938; Held and Soden, 2000). Though in the past there has been some debate as to whether or not industrialization would produce global warming or global cooling, over the past several decades the literature has increasingly favored the global warming thesis which states that significant increases in the quantity of atmospheric CO_2 results in elevated global temperatures. Accurate CO_2 measurements are available from the Mauna Loa Observatory, Hawaii from 1959. At that time CO_2 levels were 316 ppmv. Measurements now indicate CO_2 levels are 387 ppmv, an increase of 22.8% from 1958 levels. Preindustrial CO_2 levels (1850 to 1880) are estimated to have been between 260 to 290 ppmv (National Research Council, 1983; Wigley, 1983; Ramanathan et al., 1985). Because CO_2 is not chemically active it is expected to persist in the atmosphere from decades to centuries. Estimates indicate the atmosphere could undergo a CO_2 doubling from preindustrial levels sometime between 2070 and 2100.

While increased CO_2 levels are the principle cause of what is commonly called "global warming" other important greenhouse gases are also affected: ozone, water vapor, methane, and nitrous oxide. From a thermal viewpoint the dominant gases are water vapor, carbon dioxide, and ozone, followed by methane and nitrous oxide. Several authors have emphasized that water vapor is the most important greenhouse gas (Held and Soden, 2000; Soden, 2005). Water vapor is highly important to the heating and cooling mechanisms in the troposphere, which contains nearly all the atmospheric water vapor. In the middle atmosphere carbon dioxide and ozone dominate the radiative thermal properties of that region.

Atmospheric models predict that doubling the amount of atmospheric CO_2 will increase heat retention in the troposphere and increased heat loss in the stratosphere and mesosphere. Surface temperatures are expected to increase by about 1.5

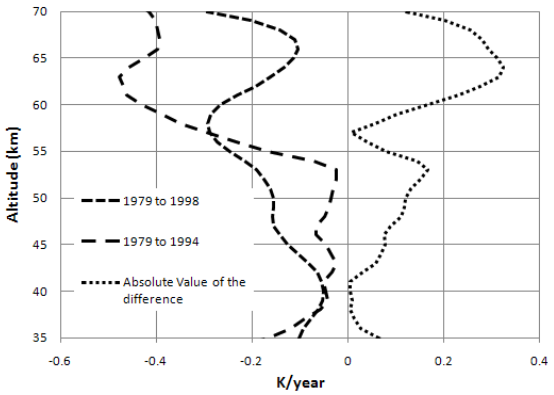

Figure 1: The figure shows a linear trend coefficient profile based on the temperature data from OHP and CEL French lidars. The profile for 1979 to 1994 is from Keckhut (1995); for 1979 to 1998 is from Ramaswamy (2001).

to 4 C while the middle atmosphere is expected to cool between 8 to 10 C for a CO_2 doubling, depending on the model simulation, location, and altitude (Rind et al., 1990, 1998; Held and Soden, 2000; Fomichev et al., 2007). Given that the middle atmosphere temperature change is expected to be about an order of magnitude greater than that in the lower atmosphere many scientists are looking for evidence of global "warming" in long term middle atmosphere temperature trends.

2 Analysis of the data

Least squares models are frequently employed as a way to extract useful information about atmospheric trends of interest, such as the quasi-biennial oscillation, the amplitude and phase of the annual oscillation and semi-annual oscillation, the atmospheric solar response, linear cooling rate, and interventions such as the Mt. Pinatubo eruption (She et al., 1998), and detecting turnaround time and recovery for ozone levels (Reinsel et al., 2002, 2005). Least squares has many advantages. It minimizes what the model cannot explain, it offers the best linear unbiased estimator (the BLUE assumption) when certain conditions are met, it is simple and the results are typically easy to analyze. Three difficulties associated with this technique are collinearity, model specification, and serial correlation. Only the first two will be considered here.

Unless otherwise stated the principle model under consideration is as follows.

$$\begin{aligned} T(z,t) = {} & \alpha(z) + \beta(z)\cdot t + \\ & A_1(z)\cos(2\pi\cdot t) + A_2(z)\sin(2\pi\cdot t) + \\ & B_1(z)\cos(4\pi\cdot t) + B_2(z)\sin(4\pi\cdot t) + \\ & C_1(z)\sin(\omega t) + C_2(z)\cos(\omega t) + \\ & D\cdot solnoise + \varepsilon(z,t) \end{aligned} \quad (1)$$

where α is the intercept coefficinet, β the linear trend coefficient, A_1 and A_2 yield the amplitude and phase of the annual oscillation, B_1 and B_2 are the same for the semi-annual oscillation, C_1 and C_2 yield the amplitude and phase of the atmospheric solar response with $\omega \sim 2\pi/11$ year^{-1}, the frequency of the solar cycle.

Occasionally a short hand notation is used to refer to a model. For example, y ~ x1 + x2 means a column **y** of data is projected on to the column space $\mathbf{X} = (\mathbf{1}, \mathbf{x1}, \mathbf{x2})$, or $\mathbf{y} = I\cdot\mathbf{1} + a\cdot\mathbf{x_1} + b\cdot\mathbf{x_2} + \boldsymbol{\varepsilon}$. In the shorthand the intercept **1**, the noise **ε**, and coefficients I, a, and b are implied. This is the notation used in the R programming language. Another short hand is sin(ω**t**) which should be taken to indicate: sin(ω**t**) = {sin ωt_1, sin ωt_2, sin ωt_3, ... , sin ωt_n}.

The solar proxy data (in this case Mg II) was downloaded from the NOAA website. A handful of missing Mg II data points were interpolated and the Mg II time series was filtered using an 81 day boxcar average. The solnoise term is obtained by fitting solar proxy data to the sin ωt and cos ωt model: MgII ~ sinωt + cosωt. The solar noise is the model residuals.

One justification for separating the solar-like oscillation from the solar noise is the possibility of a phase lag between the solar input and the atmospheric solar response. It turns out that at some altitudes the solar noise is highly correlated with the OLS residuals when the solar term is omitted. Least-squares minimizes the residual sum

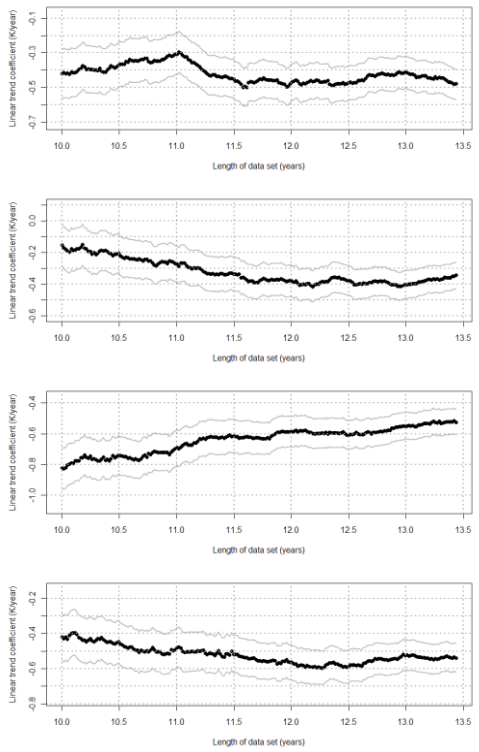

Figure 2: The time evolution of the linear trend coefficient in four different Monte Carlo simulations.

of squares (RSS), and in several exemplifying cases the solar-noise term reduced the RSS much more than the solar-like oscillation did. This means that if the terms are not separated then the reduction of the RSS by the solar noise could lead to a false positive; the amplitude of the solar proxy could be considered statistically significant when the atmospheric solar response is out of phase (and possibly attenuated) with the solar proxy. By separating these terms this problem is avoided. Additionally, the magnitude of the solar-noise coefficient may contain information about how the atmosphere is responding to solar input.

There is good reason to believe that the atmospheric solar response can be significantly out of phase with the solar input. In analyzing HALOE data Remsberg et al. (2002) found a phase lag of 2.3 years at 40º N at 0.05 hPa. They also report a lag of 1.9 and 1.5 years at 0.03 hPa and 0.02 hPa respectively, at same latitude. In an updated paper Remsberg and Deaver (2005) analyze HALOE data from 1991-2004 and found a phase lag of 3.8 years at 0.05 hPa and 2.2 years at 0.03 hPa. This is confirmed again in Remsberg (2008) which reports a phase lag of 4.5 years at 69 km and a negative phase lag between 58 and 63 km.

3 Linear trend coefficient

The value of the linear trend coefficient is one of the parameters of interest in middle atmosphere studies and is commonly used as an indicator of the magnitude of middle atmosphere cooling. But there are difficulties associated with the time evolution of the coefficient value. The following Monte Carlo simulation will illustrate the nature of this problem. A simulated temperature time series was generated containing a liner trend of −0.5 K/year and a 4 K (solar max − solar min) solar temperature response and Gaussian noise with zero mean and standard deviation of 9 K, which are realistic for mesosphere temperatures. A least squares regression is then done using this simulated time series as the response variable. As data is added to the data set the coefficient values evolve, giving us an idea of the time evolution of the linear trend coefficient. Shown in Figure 2 are the results of four different Monte Carlo runs, each starting with initially 10 years of data. The first simulation indicates a cooling trend of −0.4 K/year with ten years of data. The value of the linear trend coefficient then increases to −0.3 K/year over the period of a year. Then within a half-year it decreases to −0.5 K/year then quickly increases again to −0.4 K/year. The second simulation indicates a cooling rate of −0.15 K/year with ten years of data. The linear trend steadily decreases over the next two years to −0.4 K/year before increasing only slightly. The third simulation starts with a linear trend coefficient of −0.8 K/year which increases steadily over 3.5 years to −0.5 K/year. The fourth simulation starts with a linear trend coefficient of −0.4 K/year and decreases steadily over a period of two years to −0.6 K/year. Over the following year it then increases to −0.5 K/year.

These results indicate that the linear trend coefficient itself not only has an inherent variance that is dependant on the model specification and noise, but can also have significant temporal variation. Given enough time the linear trend coefficient will approach its true value, but

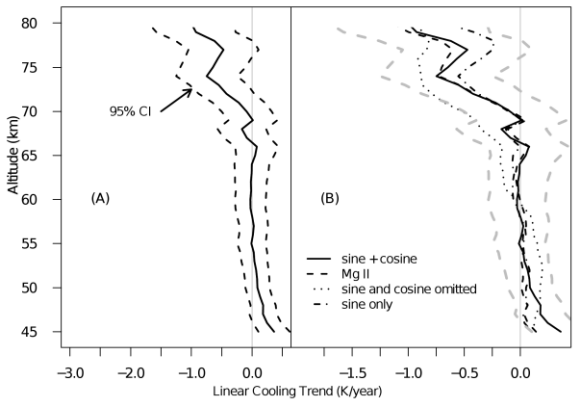

Figure 3: (A) shows the linear trend profile from Model (1). (B) shows linear trend profiles generated with various terms omitted.

convergence might not be immediate or even initially in the right direction. Linear trend coefficients from different sites can initially have very different values and very different time evolutions. As an example, Figure 1 shows the linear trend profiles from Keckhut (1995) from 1979-1994 and an updated profile of the same data set spanning from 1979 to 1998 reported in Ramaswamy (2001). The addition of four years of data noticeably alters the vertical profile. At 64 km the magnitude of the difference is 0.3 K/year, which is a rather significant amount considering that the linear trend profile itself varies from –0.2 to −0.4 K/year. One way to work around this is to compare linear trend values obtained from many different data sets. But for in situ measurements not much that can be done about the time evolution of the linear trend coefficient. One can only bring out this inherent difficulty in the data analysis process.

Another difficulty is the problem of coefficient correlation. This problem arises from the model itself and is unrelated to the temperature data. Depending on the degree of linear dependence between explanatory variables their coefficients can be correlated. In short, if two regressors are highly correlated then their coefficients are likely to be correlated.

Several of the terms in Model (1) are, unfortunately, sensitive to collinearity. Depending on the phase of the atmospheric solar response the linear trend regressor may be highly correlated with the solar-like regressors sin ωt and cos ωt. The coefficient correlations between the Model (1) regression coefficients are shown in Table 1. The correlation between the intercept and the other coefficients are of no practical interest and are omitted from the table. The highest correlation of interest is between the linear trend coefficient β and solar-like sin ωt coefficient C_1. A correlation of –0.829 when compared to the others is quite high, the next strongest correlation is +0.516 which is the correlation between β and the other solar-like coefficient C_2 corresponding to the cos ωt solar-like term. The negative correlation indicates an inverse relationship: If the linear trend coefficient happens to be higher than the true value then the coefficient C_1 is likely to be low; conversely, if the linear trend value is low then C_1 will likely be high. The converse is true for a positive correlation. Because these values are coupled a joint interpretation is normally necessary.

Another test was conducted to check for coefficient sensitivity to model specification. Regressions were done with both the sine and cosine solar-like terms omitted, with the Mg II term in place of the solar-like terms, with both solar-like terms included, and with the sin ωt term only. With the exception of the regression that included the Mg II term all the other models employed a solar noise term. It was found that with the exception of the model with both solar-like terms omitted there was not much variation in the linear terms below 75 km. However, all the variations were confined to the 95% confidence levels of the linear term from model (1). Consideration of the linear trend coefficient values

may then be confined to the region of the error bars shown in Figure 3 (A) and (B).

What is striking is the very large linear cooling rate in the upper mesosphere, ~ −1 K/year at 80 km. In a review of mesospheric temperature trends Bieg et al. (2003) lists many of the trends found by other researchers. A histogram of these trends for the mesosphere and mesopause is given in Figure 6. The median of the mesosphere trends are approximately −0.35 K/year; at the mesopause level it is approximately −0.05 K/year. There are two cases where the linear cooling rate was ~ 10 K/year. These trends were reported by Resin and Scheer (2002) reporting on airglow intensities from Argentina, and Golitsyn et al. (1996) reporting on Russian rocketsonde data.

	β	A1	A2	B1	B2	C1	C2	D
β	1.000	-0.173	0.191	0.078	-0.045	-0.829	0.516	-0.011
A1	-0.173	1.000	-0.222	-0.01	-0.199	0.215	0.139	0.077
A2	0.191	-0.222	1.000	0.107	0.233	-0.106	-0.044	0.048
B1	0.078	-0.010	0.107	1.000	-0.001	0.016	0.119	-0.065
B2	-0.045	-0.199	0.233	-0.001	1.000	-0.014	-0.041	-0.103
C1	-0.829	0.215	-0.106	0.016	-0.014	1.000	-0.413	0.024
C2	0.516	0.139	-0.044	0.119	-0.041	-0.413	1.000	-0.013
D	-0.011	0.077	0.048	-0.065	-0.103	0.024	-0.013	1.000

Table 1: The coefficient correlations for model (1). The highest correlation is between the solar-like sine term and the linear trend coefficients, 0.776. The next strongest correlation is between the linear trend coefficient and the solar-like cosign term, −0.358. The value of the intercept is not under consideration and therefore correlations between α and the other coefficients are not considered.

4 Pinatubo eruption

One possible influence on the linear trend values is the influence of the Mt. Pinatubo eruption that occurred June 9−17, 1991. This eruption produced 20 to 30 megatons of new aerosol sulfate particles, mainly from chemical reactions with sulfur dioxide (McCormick and Veiga, 1992). These particles scatter light in the visible wavelength but absorb radiation in the IR and near IR spectral regions, the net effect is heating (Thomas et al., 2009). She et al. (1998) found a 9 K and 12.9 K warming at 86 and 100 km respectively. The maximum of these warmings occurred mid 1993 at 86 km, and early 1993 at 100 km. Keckhut et al. (1995) reported a temperature increase of 2 to 3 K from 30 to 40 km from the summer of 1992 to the summer of 1993 in the residuals of their temperature data, obtained from the French CPC and OHP lidars. They also included an optical depth parameter in the linear regression model and found it to be statistically significant from 30 to 35 km and from 60 to 74 km. These two groups were fortunate enough to be taking data before and after the Pinatubo eruption permitting them to see it's before and after effects. The difficulty as it applies to the USU data is that our data set begins mid 1993, which is when the Pinatubo effect was most strongly affecting mesopause temperatures. So we expect our temperatures from that time to be perturbed higher and then rapidly drop off, but additionally we are attempting to detect a secular trend. Separating one from the other is not an easy task. If we eliminate too much of our initial data then our error increases, making results less certain.

To test for the presence of a possible temperature perturbation occurring at the beginning of the USU data, our data set was divided into two separate data sets; linear regressions were done on each. There is a one year gap occurring in 1997 so that seemed like a good place to divide the data. Let S_1 indicate the data from the first half of the data set and S_2 indicate

data from the second half of the data set. S_1 consists of 251 data points and S_2 consists of 333, at 45 km. I also excluded the solar term from the model because, owing to the shortness of S_1 and S_2, the collinearity problem was extreme, to say the least—with a sin ωt and cos ωt terms included in the model the linear term β for S_1 was −14 K/year! With the solar-like sine and cosine term omitted it was +0.45 K/year. This is clearly a case where the collinearity problem is so extreme that it was better to eliminate some model variables and risk possible bias in the linear terms. First the USU data was deseasonalized, the annual and semi-annual oscillation were removed from the data. The model that was fit to the data is then T ~ t, where t is the linear time regressor. The regression profiles for each of S_1 and S_2 are shown in Figure 5A. Below 50 km there is a significant difference between the linear trends of S_1 and S_2. At 45 km the earlier S_1

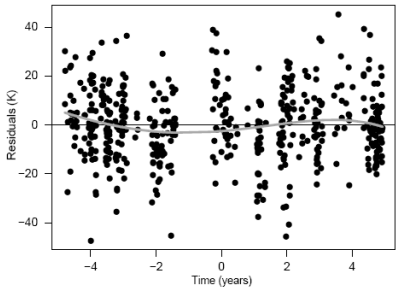

Figure 4: The residuals from fitting the model y ~ sinωt to the deseasonalized data. The gray line is a fourth order polynomial fit, added to bring out the underlying structure.

data has a warming trend of +0.39 K/year and the later S_2 data has a cooling trend of about −0.45 K/year. From 50 to 72 km they are less than 0.5 K from each other. Above 72 km they sharply diverge. Above 72 km the linear trend in the first half of the data set is on average 2 K/year greater in magnitude than the linear trend from the second half of the data set. In the upper half of the mesosphere the linear trend from September, 1993 to April, 1997 is much greater than the linear trend from May, 1998 to August, 2003.

The linear trends were also calculated for the data set with the first two years removed, so the new data set consisted of data from September, 1994 to August, 2003; here S_2 consists of 531 data points. The linear trend profile is shown in Figure 5B. While they are much closer to the linear trends for the full data set, above 50 km they are either nearly identical to the linear trends from the full data set or are slightly smaller in magnitude.

An additional difficulty is the atmospheric solar response. Most researchers have included a fixed solar proxy in the least squares model. However, if the atmospheric solar response is out of phase with the solar input and a fixed proxy in included in the model then a sinusoidal-like signal remains in the model residuals. In the case of the USU temperatures the phase of the solar cycle is such that the middle of the solar cycle is located at the time center of our data set. When y ~ time + sinωt was applied to the data there remained a significant periodical structure in the residuals. This is shown in Figure 4. In this figure the residuals from the model just mentioned are plotted. A forth order polynomial was applied to the residuals and added to the plot to emphasize the underlying structure. The temperatures at the beginning drop off quickly then slightly increase and then decrease again. This could indicate a Pinatubo effect, and unaccounted for atmospheric solar-like response, or possibly both. Also, it could simply be a periodic signal imposed on the data as a result of subtracting sin ωt from the original signal.

5 The effects of collinearity

Two effects of collinearity are increased coefficient standard errors and correlated coefficients. The effects of collinearity can sometimes be seen when a model regressor is omitted. The coefficient standard errors can change dramatically and the coefficient values themselves can also change. One effect that should be mentioned is the change in the standard error which has a direct bearing on the coefficient error limits. If one model variable is highly correlated

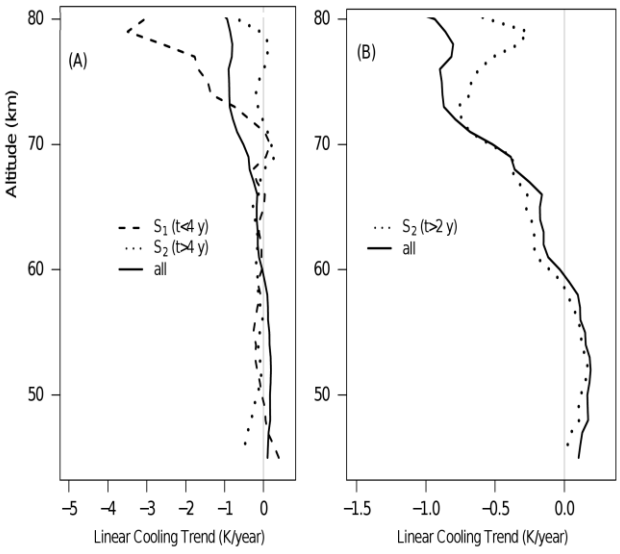

Figure 5: Comparison of linear trends from an OLS model applied to S_1 and S_2, and the entire data set. t = 0 marks the time of the first data point. (A) shows linear trends from the first and second half of the data set as well as the linear trend from the entire data set. (B) shows the linear trends for the entire data set as well as for the data set with the first two years removed.

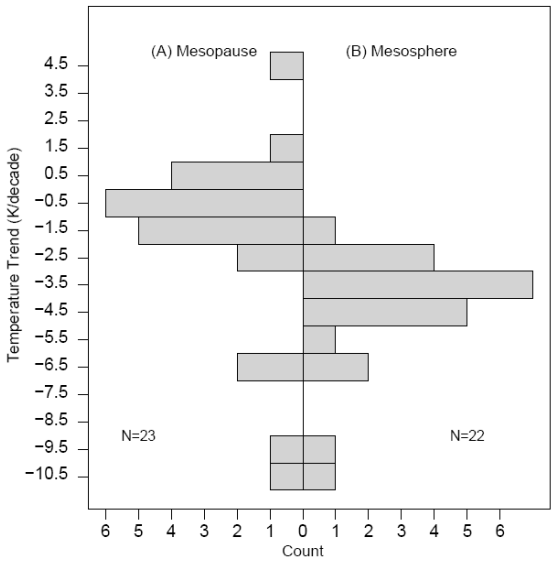

Figure 6: Histogram of temperature trends from Beig et al. (2003). (A) is for temperature trends near Mesopause 80-100 km from Beig Table 5. (B) is for trends in the mesosphere 50-79 km from Beig Table 4. For cases where the temperatures were reported as, for example, −1.4 to −2.1 K/decade both the upper and lower limits were included in the creation of the histograms. The mesopause histogram was constructed from 23 data points and the mesosphere histogram from 22.

with another the standard errors for those variables will increase. In linear regression problems a typical null hypothesis is something like, H_0: $\theta = 0$, where θ is a regression coefficient. The p value gives evidence on whether to assert or reject H_0 given the data. If the evidence strongly indicates that H_0 is false then little confidence is placed in the regression coefficient. Higher SEs increase the error bars and increase the chance of rejecting H_0.

To illustrate this several different models were fit to the data. Model (1) is y ~ time + SO + SAO + SOL + SN, where where AO is the annual oscillation, SAO is the semi-annual oscillation, SOL includes the solar-like sin ωt and cos ωt terms, and SN is the solar noise term. Model (2) is y ~ time + AO + SAO + SN. Model (2) is simply model (1) with the solar-like terms omitted. Figure 7 shows the plotted 95% CI error bars for the linear terms of (1) and (2). On average, the error bars for the model (2) are 48% smaller than the error bars for model (1). This large difference is principally due to collinearity between the linear term and the sin ωt term.

6 Summary

With the exception of the data point at 45 km there are no significant linear trends from 45 to 72 km above the 95% level. For the full model at 45 km there is a slight warming of 0.36 K/year, but if the solar terms are omitted the linear trend becomes +0.11 K/year and is significant at less than 95%. The linear term from model (2) indicates a warming from 46 to 55 km of about 0.17 K/year. For Model (1) the linear trend coefficient is not statistically significant at the 95% level from 47 to 72 km, but there is warming at 45

and 46 km of about +0.36 and +0.24 K/year. Model (1) does indicate a statistically significant cooling from 73 to 80 km, with the exception of 77 and 78 km which are only just below the 95% level. For model (2) the cooling rate has greater than 95% confidence from 62 to 80 km. The linear trend values from models (1) and (2) differ only by

There is no way to get around the fact that the cooling rate in our mesopause temperatures is larger than what most other researchers have found. The natural thing to point to is the influence of the Mt. Pinatubo eruption. Unfortunately because we do not have data before the eruption we cannot easily asses whether this is the cause of

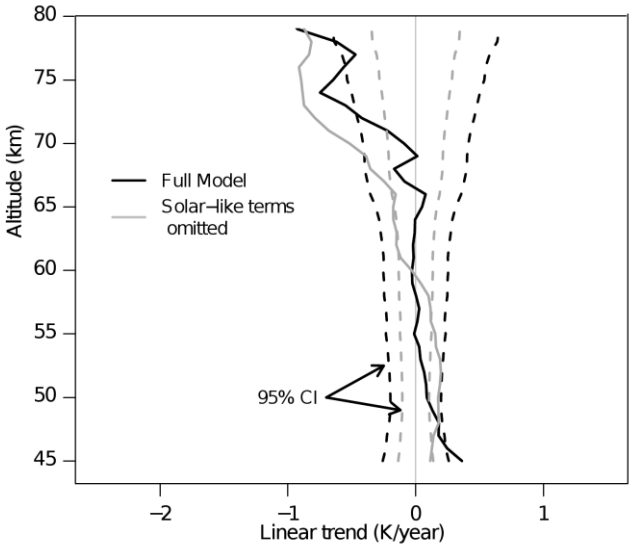

Figure 7: The linear trend coefficient profiles from model (1) and model (2) with 95% confidence levels.

a maximum value of 0.6 K/year. On average they differ by 0.2 K/year. It should also be pointed out that this upper atmosphere region is where the linear trend has its greatest uncertainty. This is partly do to increased levels of noise as well as the fact that we have fewer data points from the upper mesosphere.

Our linear mesopause trends are, needless to say, big. Comparing our results to those shown in Figure 6 one can see there are only a few data points from other groups with linear trends on the order of −1 K/year. For the mesosphere the two high cooling rates are from the Russian rocketsonde data (−8.8 and −10 K/decade). For the mesopause the high cooling rates are found in hydroxyl rotational measurements (−10.5 and −9 K/decade).

the high cooling rate obtained from the linear regressions applied to our temperature data.

We can report a statistically significant linear trend ranging from −0.5 to −1 K/year from 74 to 80 km. Below, down to about 60 km, the cooling varies between −0.5 K/year and zero. The non-zero values are not statistically significant. From 60 to 45 km there is either a zero cooling rate or slight warming of +0.36 to +0.24 K/year, depending on which model is fit to the data.

7 Additional comments

Because space limitations do not permit a further analysis and comparison of the annual and semi annual oscillations Figure 8 is given. It compares the annual and semiannual amplitudes and phases of our USU temperatures with the OHP

and CEL French lidars. The French data is from Plate 4 of Leblanc et al. (1998).

Acknowledgments: This research has been supported by Utah State University and the Rocky Mountain Space Consortium.

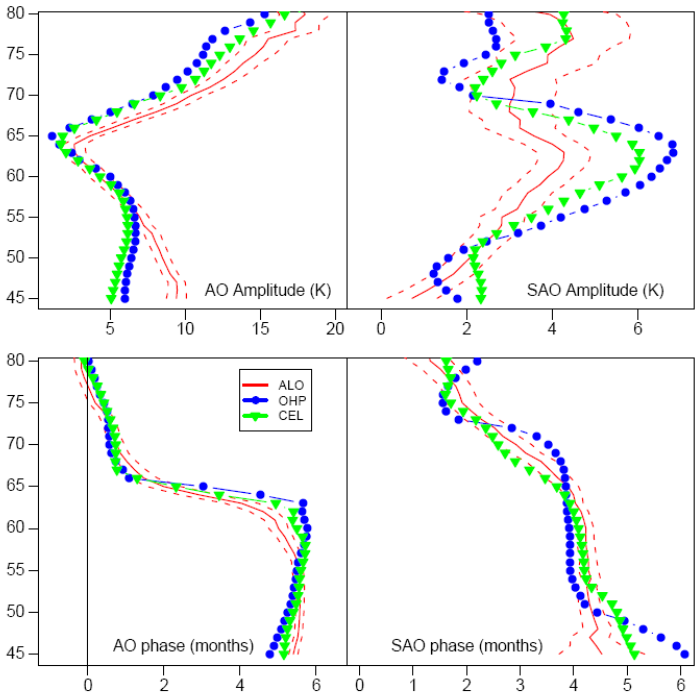

Figure 8: (A) shows the amplitude of the annual oscillation from the USU ALO lidar and the French CPC and OHP lidars. (B) shows the amplitude of the semiannual oscillation. (C) shows the phase of the annual oscillation. And (D) shows the phase of the semiannual oscillation.

References

Beig, G., 2003. Review of mesospheric temperature trends. Reviews of Geophysics 41 (4), doi:10.1029/2002RG000121.

Callendar, G. S., 1938. The artificial production of carbon dioxide and its influence on temperature. Quarterly Journal of the Royal Meteorological Society 64 (275), 223-240, doi:10.1002/qj.49706427503.

Fomichev, V. I., Jonsson, A. I., de Grandpré, J., Beagley, S. R., McLandress, C., Semeniuk, K., Shepherd, T. G., 2007. Response of the middle atmosphere to CO2 doubling: results from the canadian middle atmosphere model. Journal of Climate 20 (7), 1121, doi:10.1175/JCLI4030.1.

Golitsyn, G. S., Semenov, A. I., Shefov, N. N., Fishkova, L. M., Lysenko, E. V., Perov, S. P., 1996. Long- term temperature trends in the middle and upper atmosphere. Geophysical Research Letters 23 (14), 1741, doi:10.1029/96GL01592.

Held, I. M., Soden, B. J., 2000. Water vapor feedback and global warming. Annual Review of Energy and the Environment 25 (1), 441-475, doi:10.1146/annurev.energy.25.1.441.

Keckhut, P., Hauchecorne, A., Chanin, M. L., 1995. Midlatitude long-term variability of the middle atmosphere: Trends and cyclic and episodic changes. Journal of Geophysical Research 100 (D9), 18887–18897.

Leblanc, T., McDermid, I. S., Keckhut, P., Hauchecorne, A., She, C. Y., Krueger, D. A., 1998. Temperature climatology of the middle atmosphere from long-term lidar measurements at middle and low latitudes. Journal of Geophysical Research

103 (D14), 17191–17204.

McCormick, M. P., Veiga, R. E., 1992. SAGE II measurements of early Pinatubo aerosols. Geophysical Research Letters 19 (2), 155–158.

National Research Council, 1983. Changing climate: report of the Carbon Dioxide Assessment Committee, National Academy Press, Wachington, D.C.

Ramanathan, V., Cicerone, R. J., Singh, H. B., Kiehl, J. T., 1985. Trace gas trends and their potential role in climate change. Journal of Geophysical Research 90 (D3), 5547-5566, doi:10.1029/JD090iD03p05547.

Ramaswamy, V. et al., 2001. Stratospheric temperature trends: Observations and model simulations. Reviews of Geophysics 39 (1), 71–122.

Reinsel, G. C., Miller, A. J., Weatherhead, E. C., Flynn, L. E., Nagatani, R. M., Tiao, G. C., Wuebbles, D. J., 2005. Trend analysis of total ozone data for turnaround and dynamical contributions. Journal of Geophysical Research 110 (D16), doi:10.1029/2004JD004662.

Reinsel, G. C., Weatherhead, E. C., Tiao, G. C., Miller, A. J., Nagatani, R. M., Wuebbles, D. J., Flynn, L. E., 2002. On detection of turnaround and recovery in trend for ozone. Journal of Geophysical Research 107 (D10), doi:10.1029/2001JD000500.

Reisin, E., 2002. Searching for trends in mesopause region airglow intensities and temperatures at El Leoncito. Physics and Chemistry of the Earth, Parts A/B/C 27 (6-8), 563-569, doi:10.1016/S1474-7065(02)00038-4.

Remsberg, E. E., 2002. Seasonal and longer-term variations in middle atmosphere temperature from HALOE on UARS. Journal of Geophysical Research 107 (D19), doi:10.1029/2001JD001366.

Remsberg, E. E., 2008. On the observed changes in upper stratospheric and mesospheric temperatures from UARS HALOE. Annales Geophysicae 26 (5), 1287-1297.

Remsberg, E. E., Deaver, L., 2005. Interannual, solar cycle, and trend terms in middle atmospheric temperature time series from HALOE. Journal of Geophysical Research 110 (D6), doi:10.1029/2004JD004905.

Rind, D., Shindell, D., Lonergan, P., Balachandran, N. K., 1998. Climate change and the middle atmosphere. Part III: The doubled CO2 climate revisited. Journal of Climate 11 (5), 876–894.

Rind, D., Suozzo, R., Balachandran, N. K., Prather, M. J., 1990. Climate change and the middle atmosphere. Part I: The doubled CO2 climate. Journal of the Atmospheric Sciences 47 (4), 475-494, doi:10.1175/1520-0469(1990)047<0475:CCATMA>2.0.CO;2.

She, C., Thiel, S. W., Krueger, D. A., 1998. Observed episodic warming at 86 and 100 km between 1990 and 1997: Effects of Mount Pinatubo eruption. Geophysical Research Letters 25 (4), 497, doi:10.1029/98GL00178.

Soden, B. J., 2005. The Radiative Signature of Upper Tropospheric Moistening. Science 310 (5749), 841-844, doi:10.1126/science.1115602.

Thomas, M. A., Timmreck, C., Giorgetta, M. A., Graf, H. F., Stenchikov, G., 2009. Simulation of the climate impact of Mt. Pinatubo eruption using ECHAM5 – Part 1: Sensitivity to the modes of atmospheric circulation and boundary conditions. Atmospheric Chemistry and Physics 9, 757-769.

Wigley, T. M. L., 1983. The pre-industrial carbon dioxide level. Climatic Change 5 (4), 315-320, doi:10.1007/BF02423528.